Proceedings of the ASME 2023
International Design Engineering Technical Conferences and
Computers and Information in Engineering Conference
IDETC-CIE2023
August 20-23, 2023, Boston, Massachusetts

DETC2023-114601

DESIGN OF MIXED-CATEGORY STOCHASTIC MICROSTRUCTURES: A COMPARISON OF CURVATURE FUNCTIONAL-BASED AND DEEP GENERATIVE MODEL-BASED METHODS

Leidong Xu, Kiarash Naghavi Khanghah, Hongyi Xu*

Mechanical Engineering, University of Connecticut, Storrs, CT 06269

* Email: hongyi.3.xu@uconn.edu

ABSTRACT

Bridging the gaps among various categories of stochastic microstructures remains a challenge in the design representation of microstructural materials. Each microstructure category requires certain unique mathematical and statistical methods to define the design space (design representation). The design representation methods are usually incompatible between two different categories of stochastic microstructures. The common practice of pre-selecting the microstructure category and the associated design representation method before conducting rigorous computational design limits the design freedom and reduces the possibility of obtaining innovative microstructure designs. To overcome this issue, this paper proposes and compares two methods, the deep generative modeling-based method and the curvature functional-based method, to understand their pros and cons in designing mixed-category stochastic microstructures for desired properties. For the deep generative modeling-based method, the Variational Autoencoder is employed to generate an unstructured latent space as the design space. For the curvature functional-based method, the microstructure geometry is represented by curvature functionals, of which the functional parameters are employed as the microstructure design variables. Regressors of the microstructure design variables-property relationship are trained for microstructure design optimization. A comparative study is conducted to understand the relative merits of these two methods in terms of computational cost, continuous transition, design scalability, design diversity, dimensionality of the design space, interpretability of the statistical equivalency, and design performance.

Keywords: Stochastic microstructures; Microstructure design; Deep generative model; Curvature functional; Design representation.

1. INTRODUCTION

By designing the microstructures of architected materials, a wide spectrum of properties, such as strength [1-3], ductility [4], energy density [5, 6], and thermal conductivity [1, 7, 8], can be achieved to meet engineering requirements. Here we focus on stochastic microstructures, of which the statistical variations in structural characteristics are induced by uncertainties in the manufacturing processes [9-11], defects or porosities [12], or the inherent randomness at the micro- or nano-scale [13, 14]. In the field of engineered architected metamaterials, designers have looked into stochastic structure designs to achieve higher energy absorption [6, 15, 16], compatibility with traditional manufacturing techniques [17, 18], and robustness against defects [19].

In the literature, a variety of statistical characterization and stochastic reconstruction-based approaches have been proposed for designing stochastic microstructures. Statistical characterization is a process that generates statistical descriptors and functions of the stochastic microstructure features observed from digital images (e.g., microscopic images). Stochastic reconstruction is a process that re-generates statistically equivalent microstructures based on the input statistical descriptors and functions. One simple and straightforward way is to characterize microstructures with physically meaningful parametric descriptors such as volume fraction, particle/pore size, fiber length, fiber orientation, etc. In addition, high dimensional statistical functions including N-point correlation functions [20-23], spectrum density function [24, 25], and random fields [26, 27] have also been applied to describe the complex stochastic microstructure morphologies. One major limitation of these methods is that each stochastic microstructure category requires some unique mathematical and statistical representations that are incompatible with other categories. For

example, random fiber composites require fiber orientation tensor [10, 28], random particle composites require the statistical distribution of particle diameters [29, 30], granular alloy microstructures require both grain orientation and crystal orientation [31], and spinodal-like structures can be described with spectrum density function [25]. Therefore, a designer needs to decide the microstructure category before defining the design space and conducting computational design. The step of pre-selecting the microstructure category limits the design freedom and reduces the possibility of obtaining innovative microstructure designs.

In recent years, deep generative models, such as Variational Autoencoders (VAEs), generative adversarial networks (GANs), and their variations, have been employed in stochastic microstructure reconstruction and design [16, 32-38]. However, the aforementioned works only consider a limited number of microstructure categories [39] and do not focus on bridging the gaps among various categories. In our previous work [40], we established a deep generative modeling framework that learns a unified microstructure design space based on multiple categories of stochastic microstructures (random fibers, random particles, random ellipses, random node-edge networks, and random amorphous microstructures) and deterministic, periodic microstructures (e.g., cellular metamaterials). This framework enables a smooth transition between stochastic and deterministic structural patterns in the property-driven microstructure design. However, this framework only handles 2D microstructure images and is demanding on training data and computational resources, so its application to 3D microstructure design is limited by the curse of dimensionality.

To address the aforementioned challenges, here we investigate two approaches that have the capability of generating a unified design space that embodies various categories of stochastic microstructures:

(i) A data-driven approach based on the deep generative model;

(ii) A mathematics-based approach that is established upon the curvature functionals.

As shown in **Figure 1**, these two methods are employed in design representation to create a parametric design space for stochastic microstructure design. With the obtained design space, Design of Experiments (DOE), supervised learning of the microstructure-property relationship, and property-driven design will be conducted to generate new microstructure designs. A comparative study will be presented to discuss the pros and cons of the two methods.

The remainder of the paper is organized as follows. Section 2 introduces a deep generative model-based design methodology. Section 3 introduces the curvature functional-based design methods. In section 4, a microstructure design case is presented to compare the two methods. Section 5 presents a comprehensive discussion of the comparison of the two methods. Section 6 concludes this paper.

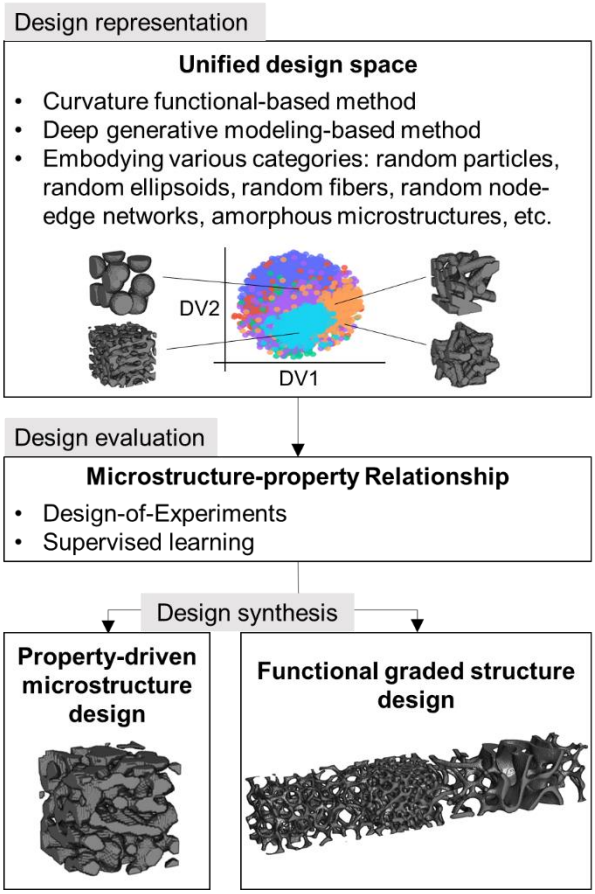

Figure 1: Design of mixed-category stochastic microstructures. The focus of this paper is to compare the curvature functional-based and the deep generative model-based methods in the design representation. Both methods will be employed to create a unified design space that embodies various categories of stochastic microstructures for the property-driven microstructure design.

2. DEEP GENERATIVE MODEL-BASED METHOD

One way to bridge the gap among different microstructure categories is to leverage the data-driven approach, e.g., deep feature learning, to learn a unified design space based on a large and diverse microstructure database that embodies various categories of microstructures. We first established a 3D stochastic microstructure database by leveraging the stochastic reconstruction methods proposed in our previous works, including the statistical descriptor-based method [10, 30, 41, 42], the space tessellation-based method [9], the spectrum density function (SDF)-based random field method [14], etc. This database consists of 40,000 microstructural images with a resolution of 64×64×64, and the microstructure samples can be classified into five categories: random particles, random fibers, random ellipsoids, random node-edge networks, and amorphous microstructures. Samples from each category are shown in **Figure 2**. The dataset is divided into a training set and a test set in a ratio of 9:1.

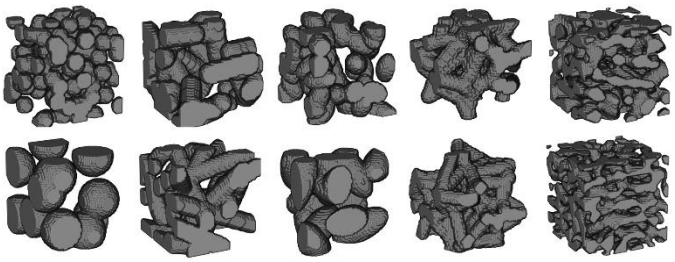

Figure 2: Examples of microstructure samples in the database for deep generative modeling. From left to right: random particles, random fibers, random ellipsoids, random node-edge networks, and amorphous microstructures.

2.1. Microstructure representation by VAE

VAE is a deep generative model that consists of two major components: an encoder network and a decoder network. The encoder network maps the input data to a Gaussian distribution in the latent space, which allows for the generation of novel data samples through sampling from the learned distribution. The decoder network takes the latent representation as the input and reconstructs the original data. The key feature of VAE is the introduction of a probabilistic approach to encode the input data into the latent space. Rather than mapping the input data to a single point in the latent space, the VAE maps the input data to a probability distribution over the latent space. Compared to other generative models, e.g., GAN and diffusion model, VAE provides an interpretable latent space, which can be used as a low-dimensional design space. The similarity of structural features can be measured by the distance in the latent space of VAE. Moreover, GAN models suffer from diminished gradient, model collapse, and other training instability issues that limit their application to complex datasets, such as mix-category microstructure datasets. Therefore, VAE is selected in this study. A general loss function of a vanilla VAE is expressed as:

$$L_i(\boldsymbol{\theta}, \boldsymbol{\phi}) = -E_{\boldsymbol{z}\sim \boldsymbol{q_\theta}(\boldsymbol{z}|\boldsymbol{x}_i)}\left[log\, \boldsymbol{p_\phi}(\boldsymbol{x}_i \mid \boldsymbol{z})\right] + D_{KL}\left(\boldsymbol{q_\theta}(\boldsymbol{z} \mid \boldsymbol{x}_i)\middle|\boldsymbol{p}(\boldsymbol{z})\right) \quad (1)$$

where $\boldsymbol{\theta}$ and $\boldsymbol{\phi}$ are the parameters of the decoder and encoder, respectively, and $\boldsymbol{x}_i$ is input microstructure image data for our case, and $\boldsymbol{z}$ denotes the latent vectors. The first term, $-E_{\boldsymbol{z}\sim \boldsymbol{q_\theta}(\boldsymbol{z}|\boldsymbol{x}_i)}\left[log\, \boldsymbol{p_\phi}(\boldsymbol{x}_i \mid \boldsymbol{z})\right]$, is the reconstruction loss that measures the pixel-level error between the input and reconstruction. The second term, $D_{KL}\left(\boldsymbol{q_\theta}(\boldsymbol{z} \mid \boldsymbol{x}_i)\middle|\boldsymbol{p}(\boldsymbol{z})\right)$, denotes the KL loss and ensures that the learned distribution q follows the true prior distribution p. Practically, including the KL term in the loss function can avoid overfitting and also regularize the latent space to reduce discontinuities in the latent space.

Figure 3 shows our implementation of the VAE to generate a parametric latent space representation of the stochastic microstructures as the design space. The encoder follows a VGG-style architecture, in which the convolution layer blocks are followed by the fully connected layers. The dimension of latent vectors is set at 256 based on the results of trials, in order to balance the reconstruction quality and the time efficiency of conducting optimal microstructure search in the latent space.

We also explored other variants of VAE in this work. Literature and our previous work suggest that including a style loss term in the loss function typically enhances reconstruction quality significantly [40, 43]. However, the small improvement in quality comes at the cost of a substantial increase in computational complexity due to the tensor permutation process on each image. We also tested an architecture that incorporates the style loss [43], but did not observe an improvement in the reconstruction quality. Furthermore, we experimented with a Gaussian-mixture VAE [44], but did not observe any significant benefits either. After a thorough exploration of these options, we decided to employ a vanilla VAE for its computational efficiency.

2.2 Property-driven microstructure design and generation of functionally graded structure designs by VAE

As discussed in Section 1, we adopt the surrogate model-based optimization approach to design microstructures for desired properties. The latent variables are considered as microstructure design variables. DOE is conducted in latent space to generate a dataset for training the microstructure-property surrogate models. Multi-response Gaussian Process (GP) regression models are employed to establish the relationship between the latent variables and the mechanical properties.

As the computational cost of design evaluation (by surrogate model) during the optimization process is not a concern here, we select the Genetic Algorithm (GA) to solve the design problem. GA, and other evolutionary algorithms, have the advantage of avoiding local minima. For multi-objective optimization problems, Non-dominated Sorting Genetic Algorithm II (NSGA-II) [45] is employed as the optimizer.

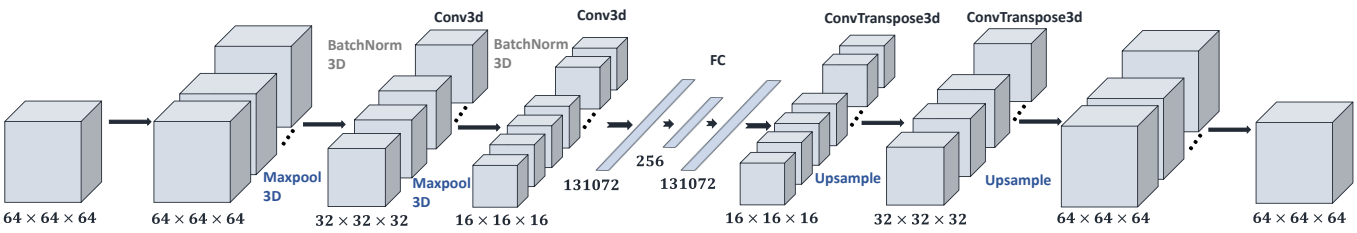

Figure 3: Architecture of the Variational Autoencoder. The reduced dimensional latent space is employed as the design space.

The optimal designs are first obtained in the format of latent vector, and the corresponding microstructure images are reconstructed by the decoder. The properties of the optimal microstructure designs are verified by simulations, as there always exist discrepancies between the surrogate model-predicted properties and the true values.

In addition to designing microstructure units, we also investigate the VAE model's capability of generating functionally graded structure designs. A functionally graded structure is characterized by the variation in structure gradually over volume, resulting in corresponding continuous changes in the properties. A series of microstructure units are generated by conducting spherical linear interpolation [46] between two microstructure unit samples in the latent space. A gradual change in the microstructure features can be observed in this series of designs. A functionally graded structure can be generated by assembling those microstructure units sequentially (**Figure 4**). Due to the discrete nature of the microstructure interpolation, one outstanding shortcoming is the lack of continuity at the interface between two adjacent microstructure units. The presence of discontinuities at the interface can lead to local stress concentrations that may weaken the overall strength of the structure and even cause it to failure. Non-smooth transitions in the interfaces can be observed, as shown in the side views in **Figure 4 (d)**.

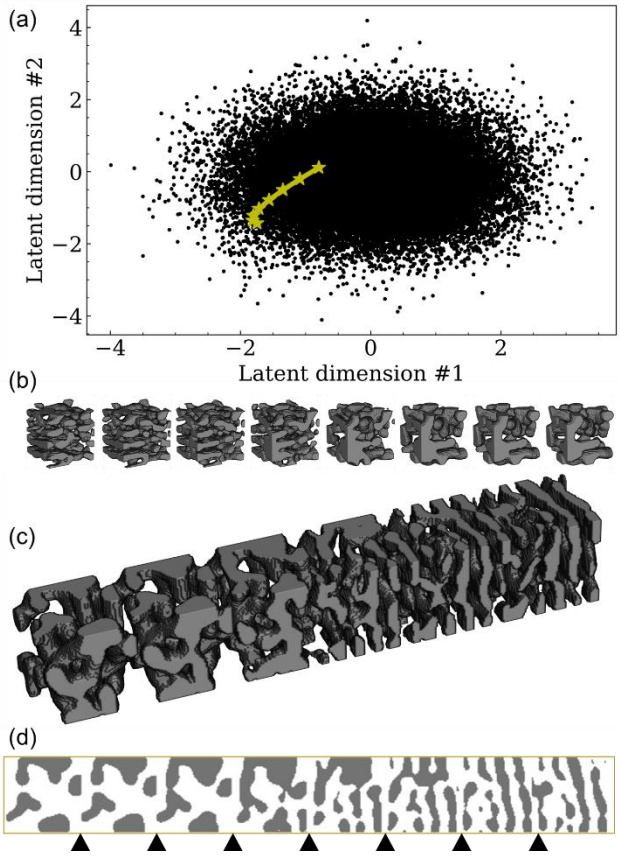

Figure 4: Functional graded structure design by the deep generative modeling-based method. (a) A series of designs are generated along a certain path in two selected dimensions of the 256-dimensional latent space. (b) Each star in the path is decoded into a microstructure unit. (c) A functionally graded structure design is created by assembling the microstructure units. (d) Side view of the 3D functionally graded structure. The interfaces among adjacent units are marked by triangles. Due to the discrete nature of the sampling process, non-smooth transitions can be observed at the interfaces among microstructure units.

3. CURVATUAL FUNCTIONAL-BASED METHOD

3.1. Microstructure representation by curvature functionals

Curvature functionals are capable of generating a variety of complex shapes and have been demonstrated as a powerful tool for designing bio-mimetic scaffold [47]. Curvature functionals employ a phase-field formulation to diffuse an approximation of a vast range of shape textures. The resulting approximation is used as a loss function, in conjunction with modern automatic differentiation optimizers, to generate geometries from a random field initialization. When compared to the phase-field [48, 49] and statistical functional approaches [25], such as spinodal microstructures generated by Gaussian random field (GRF) [2, 50], curvature functionals have the ability to generate a broader range of topologies. These include laminar, spherical, pearly thin wall, and tube shapes, and are governed by seven generation parameters $\boldsymbol{a} = [a_{2,0}, a_{0,2}, a_{1,1}, a_{1,0}, a_{0,1}, a_{0,0}]$ and m_0. However, the mathematical meaning of the generation parameters is yet fully explored which limits the capability in directly using this method for inverse design. To address this limitation, we utilize the supervised learning method to establish the relation between generation parameters and properties to enable the property-driven microstructure design.

Gaussian curvature is a differential geometry measure of the curvature of a surface at a given point, which is defined as the production of the principal curvatures κ_1, κ_2 by

$$K = \kappa_1 \kappa_2 \tag{2}$$

The complex microstructure surface under constant volume is modelled as a curvature functional

$$\boldsymbol{F}(S) = \int_S p(\kappa_1, \kappa_2) dA \tag{3}$$

where p is the second order polynomial of the principal curvatures of the entire surface S. p is restricted at the degree of 2, as it is efficient to generate topological features. The curvature functionals can be expanded as

$$\boldsymbol{F}(S) = \int_S \left(a_{2,0}{\kappa_1}^2 + a_{1,1}\kappa_1\kappa_2 + a_{0,2}{\kappa_2}^2 + a_{1,0}\kappa_1 + a_{0,1}\kappa_2 + a_{0,0}\right) dA = \int_S \left(\sum_{|\alpha|\leq 2} a_\alpha (\kappa_1\kappa_2)^\alpha\right) dA \tag{4}$$

Generally, it is convenient to refine this kind of 2D surface functionals to scalar fields u in 3D volume by diffusion approximation. And the matrix field $\mathcal{M}_u^\epsilon$ is introduced as:

$$\mathcal{M}_u^\epsilon = -\epsilon \,\mathrm{Hess}\, u + \frac{W'(u)}{\epsilon} n_u \otimes n_u \tag{5}$$

whose trace is equal to

$$\mathrm{Tr}\mathcal{M}_u^\epsilon = -\epsilon \Delta u + \frac{W'(u)}{\epsilon} \tag{6}$$

Applied phase-field approximation and further simplification, the final representation of the phase-field $\mathcal{F}_\epsilon(u)$ can be written as

$$\mathcal{F}_\epsilon(u) = \int_\Omega \left[\frac{a_{2,0}+a_{0,2}-a_{1,1}}{2\epsilon}\|\mathcal{M}_u^\epsilon\|^2 + \frac{a_{1,1}}{2\epsilon}(\mathrm{Tr}\mathcal{M}_u^\epsilon)^2 + \frac{a_{2,0}-a_{0,2}}{2\epsilon}\mathrm{Tr}\mathcal{M}_u^\epsilon\sqrt{(2\|\mathcal{M}_u^\epsilon\|^2 - (\mathrm{Tr}\mathcal{M}_u^\epsilon)^2)^+} + \frac{a_{1,0}+a_{0,1}}{2}|\nabla u|\mathrm{Tr}\mathcal{M}_u^\epsilon + \frac{a_{1,0}-a_{0,1}}{2}|\nabla u|\sqrt{(2\|\mathcal{M}_u^\epsilon\|^2 - (\mathrm{Tr}\mathcal{M}_u^\epsilon)^2)^+} + a_{0,0}\epsilon|\nabla u|^2\right]dx \quad (7)$$

To implement the phase-field $\mathcal{F}_\epsilon(u)$ to generate microstructure geometries given a random initialization, a mass-preserving flow can be defined as

$$\dot{u} = \Delta\frac{\partial \mathbb{F}_\epsilon}{\partial u} \quad (8)$$

This form can also be repressed as

$$u = \nabla\cdot A + m_0 \quad (9)$$

where $A: \Omega \to \mathbb{R}^3$ is a periodic vector field, and $m_0 \in \mathbb{R}$ is the desired value of the average $\bar{u}$ which also approximates the volume fraction by $\frac{m_0+1}{2}$. Finally, an energy function is defined as:

$$G_\epsilon(A) = \mathcal{F}_\epsilon(\nabla\cdot A + m_0) \quad (10)$$

with a gradient of

$$\frac{\partial G_\epsilon}{\partial A}(A) = -\nabla\frac{\partial \mathbb{F}_\epsilon}{\partial u}(u) \quad (11)$$

This energy function is used as the loss function with an auto-differentiation tool that iteratively optimizes u to evolve a random vector field A_0 until the energy function meets the convergence criterion. Empirically, A_0 can be drawn from a uniform distribution. Random initialization of the structure image in the curvature functional method results in diverse yet statistically equivalent stochastic reconstructions of microstructures that share the same input generation parameters $\boldsymbol{a}$ and m_0. Therefore, the generation variables can be considered as a quantitative representation of an infinite set of random but statistically equivalent microstructures, which makes this method suitable for generating random but statistically equivalent stochastic microstructure designs. Several examples of statistically equivalent microstructure samples generated from the same $\boldsymbol{a}$ vector are shown in **Figure 5 (a~d)**.

3.2 Property-driven microstructure design and generation of graded functional structure designs by curvature functionals

Following the flowchart in **Figure 1**, we propose a surrogate model-based optimization approach for microstructure design. The surrogate model of the relationship between the generation parameters $\boldsymbol{a}$ and material property is established using GP regression. It is to be noted that random but statistically equivalent microstructures will be generated for a given set of design variables. Therefore, we generated ten samples from ten fixed random initializations (A) for the same design variable vector, and then simulated the mechanical properties of all ten samples. We generated a total of 20,000 samples using 2,000 sets of generation parameters. Similar to the method presented in Section 2, we adopt GA and NSGA-II as the optimizer to solve the property-driven design problem. In the last step, the digital images of the microstructure designs are reconstructed based on the design variable vector $\boldsymbol{a}$.

Here we also investigated the curvature functional-based method's capability of generating functional graded structure designs. One advantage of the curvature functional method is that a smooth transition between different categories of microstructures can be easily obtained by varying the values of the generation parameters continuously. **Figure 5(e)** shows a functional graded design generated based on continuous functions of the generation parameters $\boldsymbol{a}$ along the longitudinal direction.

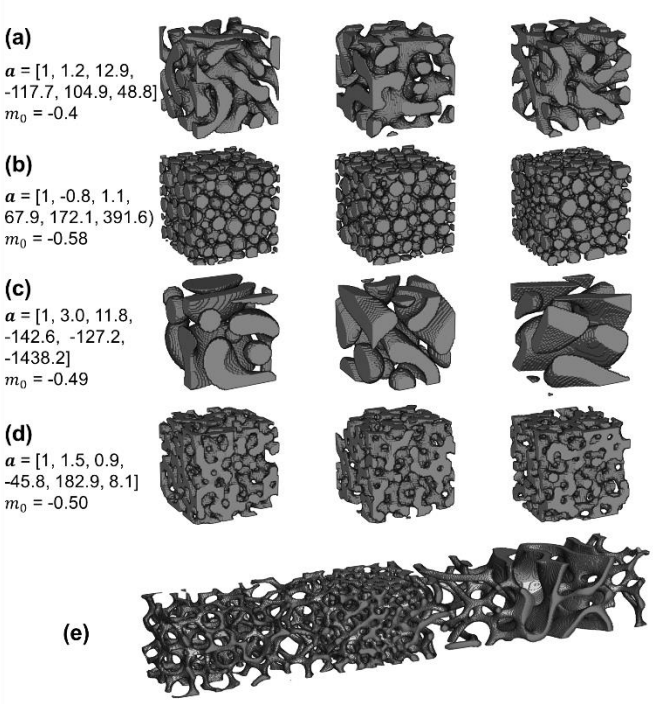

Figure 5: (a)~(d) Design variable vectors and the corresponding statistically equivalent microstructure samples. Each row shows three stochastic samples of the same microstructure design and the corresponding generation parameters. (e) A functionally graded structure obtained by the curvature functional-based method. It is created from continuous functions of the generation parameters $\boldsymbol{a}$.

4. A COMPARATIVE STUDY WITH A DESIGN FOR STIFFNESS PROBLEM

In this section, we present a design case to compare the deep generative model-based and the curvature functional-based design representation methods in two aspects: the accuracy of the microstructure-property regressor and the performance of the optimal designs obtained with each method.

Here we define a multi-objective microstructure design problem that maximizes the Young's moduli along X-, Y-, and Z- directions. Design constraints are defined to guarantee close-to-isotropic designs, i.e., the differences between the maximum/minimum modulus and the median modulus of the

three directions are within 3%. Therefore, the optimization problem can be formulated as

$$\max\ E_i(\boldsymbol{z})\ \text{or}\ \max\ E_i(\boldsymbol{a}, m_0\ ),\ i = \mathrm{X,Y,Z} \tag{12}$$

subject to:

$$\frac{|E_{\text{highest}} - E_{medium}|}{E_{medium}} < 3\% \tag{13}$$

$$\frac{|E_{\text{lowest}} - E_{medium}|}{E_{medium}} < 3\% \tag{14}$$

If using the curvature functional-based method, additional constraints are needed to guarantee the convergence of microstructure image reconstruction:

$$\max(u) > 0.1 \tag{14}$$

$$\min(u) < -0.1 \tag{15}$$

$$\text{discrepancy}(u) < 0.75 \tag{16}$$

where the discrepancy is a measurement of how much the scalar fields u deviate from a tanh profile phase field function [47]. As this research focuses on investigating the influence of microstructure morphology on the properties, the volume fraction is set as a constant (0.4).

As a preparation for exploring the relationship between microstructure and the property of interest, in this case, elasticity, we performed finite element simulations on all microstructure samples by ABAQUS. The 0-1 matrices that represent the binary microstructure images are transformed into hexahedral meshes. The elastic modulus and Poisson's ratio of the 1 phase in the microstructure are $E_{Boron} = 379300$ MPa and $\gamma_{\text{Boron}} = 0.1$, whereas $E_{\text{Aluminum}} = 68300$ Mpa, $\gamma_{\text{Aluminum}} = 0.3$ for the 0 phase. The Young's moduli (E_x, E_y, E_z) in the X-, Y-, and Z-direction are calculated from the compliance matrix. The infinitesimal displacement boundary conditions are shown in **Figure 6**.

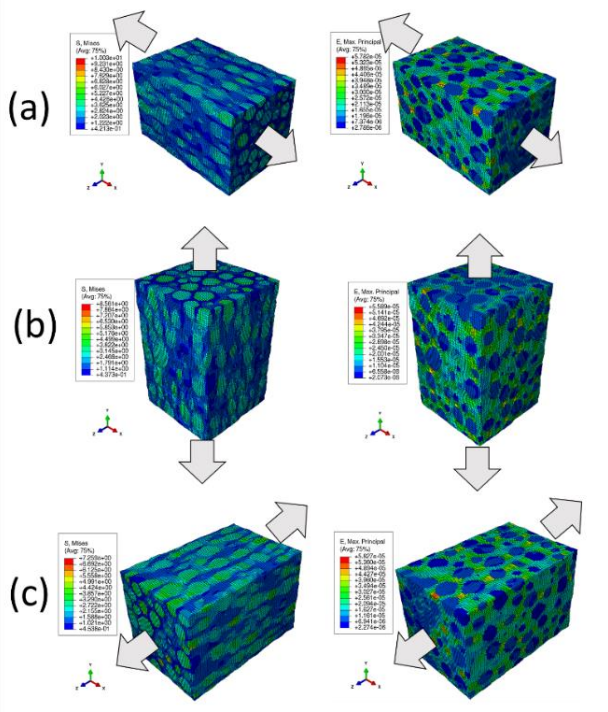

Figure 6: Elasticity property analysis on a microstructure for the maximum in-plane strain and the maximum von Mises stress in (a) X-direction, (b) Y-direction, and (c) Z-direction.

The dimensionality of the design space has a strong impact on the predictability of the GP regressors. The design space generated by VAE has a dimensionality of 256. By contrast, the design space of the curvature functional-based method is only 7. More input variables indicate a potentially better capability to capture complex microstructure features, but practically, a high dimensional input space poses a significant challenge to establishing the design variable-property relationship by surrogate modeling because a lot more training data points are required to fully cover the input space. In **Table 1**, we present a comparison of three GP models: VAE latent space-based GP model with a dataset of 40000 samples, VAE latent space-based GP model with a dataset of 20000 samples, and curvature functional-based GP model with a dataset of 20000 samples. In each training, the dataset is split into a training set (90%) and a test set (10%). The model accuracy, R^2, is evaluated based on the test set. The curvature functional-based GP model has a higher accuracy, even when comparing with the VAE-based GP model that uses twice as many training data points.

Table 1: Prediction accuracies of the GP regression models with the design spaces generated by the VAE-based method and the curvature functional-based method.

Model (size of the dataset)	R^2 score		
	E_x	E_y	E_z
GP w/VAE (40000)	0.743	0.681	0.746
GP w/VAE (20000)	0.686	0.620	0.688
GP w/ curvature functional (20000)	0.811	0.803	0.775

Another point worth noting is that some combination of generation parameters in the curvature functional method may generate ill-posed geometric which may have zero level set and floating fragments, where such fragments can lead to unrealistic microstructures in composite material and porous material from both design and manufacturing perspectives. Therefore, three criteria, $\max(u)$, $\min(u)$, and discrepancy ratio, are required to identify ill-posed phase-field u during the optimization process. These three criteria must be included as inequality constraints in optimization to ensure successful reconstructions of the final microstructure designs. Experimentally, we observe that these three constraint functions limit the number of feasible designs significantly.

The Pareto frontiers obtained with the two methods are compared in **Figure 7**. The performances of the design points in these plots are the true values obtained from verification simulations. Due to the predicted errors of the microstructure-property model, some of the optimal designs violate the design constraints on isotropicity. For the VAE-based method, only 10% of the optimal designs in the Pareto frontier satisfy the design constraints. Among the feasible designs, we can hardly find designs that rank in the top 10% compared to the samples in

the microstructure database, with respect to the properties of interest.

On the other hand, more than 70% percent of optimal designs found by the curvature functional approach are isotropic, according to the results of verification simulations. Furthermore, almost all of the feasible solution rank in the 10% compared to the samples in the microstructure database. **Figure 8 (a)~(d)** show several examples of the optimal designs obtained by the curvature functional-based method, and **Figure 8 (e) and (f)** show the optimal designs obtained by the VAE-based method.

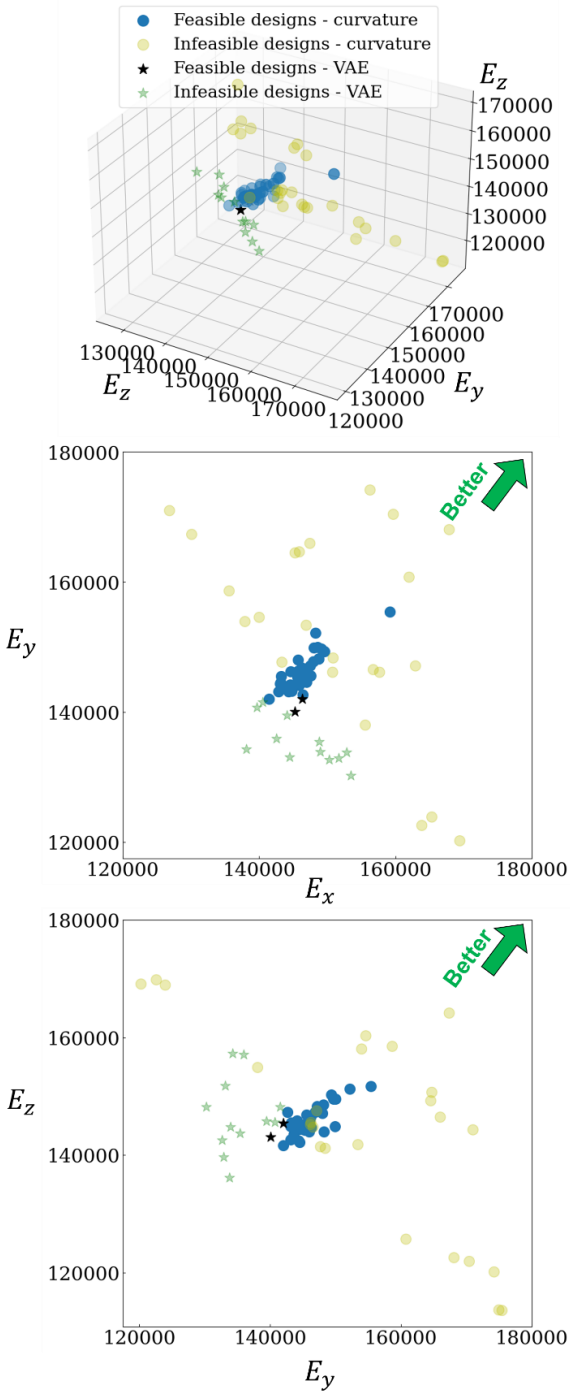

Figure 7: Pareto frontiers obtained by both design approaches. As there are three design objectives, one 3D view and two 2D views of the performance space are provided. The design objective is to maximize E_x, E_y, and E_z. The feasible design points are in dark colors and the infeasible design points are in light colors.

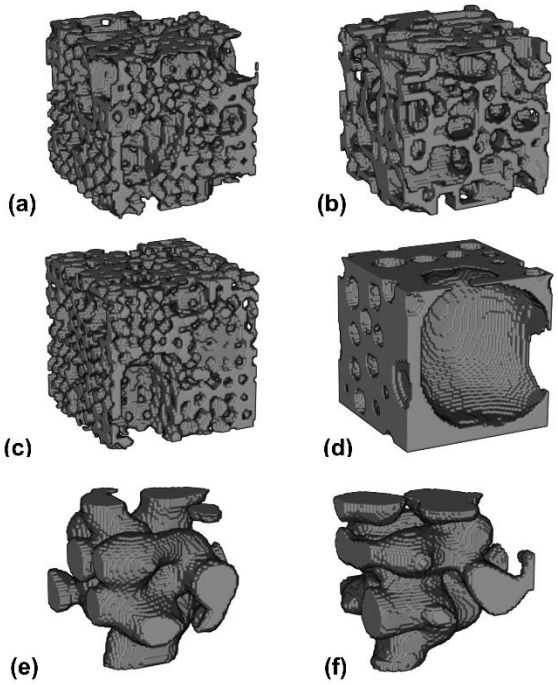

Figure 8: (a)~(d) Optimal designs from the curvature functional-based optimization approach. (a) $\boldsymbol{a}$ = [1, 4.0, 0.3, 75, 200, -2060] and m_0 = -0.26. (b) $\boldsymbol{a}$ = [1, 3.93, 3.79, 36, 194, 2998] and m_0 = -0.43. (c) $\boldsymbol{a}$ = [1, 3.99, 0.34, 45, 197, 1422] and m_0 = -0.19. (d) $\boldsymbol{a}$ = [1, 3.98, 0.22, 40, 198, 1431] and m_0 = -0.30. (e) and (f) Two optimal designs from the VAE-based design approach.

5. UNDERSTANDING THE PROS AND CONS OF THE TWO DESIGN REPRESENTATION METHODS

As summarized in **Table 2**, the pros and cons of the deep generative modeling-based method and the curvature functional-based method are discussed in terms of seven criteria: computational cost, continuous transition in functionally graded structure design, scalability of the microstructure design, design diversity, dimensionality of the design space, and design performance.

Computational cost: To obtain a design space that embodies various categories of microstructures, the deep generative modeling-based approach requires significant computing resources for data generating and model training. On the other hand, the curvature functional-based method incurs minimal costs in defining the design space, while computing the viability constraints (Equation 14~16) during the optimization process is relatively computationally expensive.

Continuous transition in functionally graded structure design: When creating functionally graded structure designs, the curvature functional-based method can guarantee a smooth transition among various microstructure patterns. With the deep generative model-based method, the functionally graded structure design is created by assembling a series of microstructure units, which correspond to discrete points in the latent space. Therefore, a smooth transition between microstructure units cannot be guaranteed. This issue could potentially be mitigated (but not resolved) by applying circular spatial padding to the transposed convolutional layer in the deep generative model [51], but the impacts on reconstruction quality and computational complexity need further investigation.

Scalability of the microstructure design: The deep generative models, which are trained on the images directly, cannot generate images with a wide range of sizes and resolutions. By contrast, the curvature functional-based method can easily map the design variables to an arbitrary domain size (**Figure 9**).

Design diversity: The deep generative models have the advantage over the curvature functionals. Theoretically, the deep generative models can be extended to embody any type of microstructure (e.g., microstructures with triangular inclusions) as long as the training data are available. The curvature functionals can only generate microstructures with curved surfaces.

Dimensionality of the design space: The curvature functional-based method has the advantage in generating a low dimensional design space. Although we can also set the dimensionality of the VAE latent space to a very low value (e.g. 8, the same as the design space of the curvature functional method) by modifying the fully connected layers in encoder, in practice, it will lead to a much poorer reconstruction accuracy. The high dimensionality of the VAE latent space poses a significant challenge to establishing the microstructure-property relationship, as well as searching for the optimal microstructure designs in the design space.

Interpretability of statistical equivalency among stochastic microstructure designs: It is a unique requirement for stochastic microstructure design. From the perspective of statistical characterization and stochastic reconstruction, one "design" actually represents an infinite number of microstructure samples that are random but statistically equivalent. The design representation by curvature functional parameters can provide this capability. By contrast, in the latent space learned by the deep generative model, each point corresponds to one specific, unique microstructure image. The distance between the points is a measurement of the pixel-to-pixel similarity of the two images, instead of the similarity in the statistical sense. As shown in **Figure 10**, two statistically equivalent random particle microstructure samples are far apart in terms of the Euclidean distance in latent space, while the random particle microstructure #1 is closer to the quasi-random microstructure. Therefore, it is not possible to define statistical equivalency purely based on the distance in the latent space. We acknowledge the possibility of generating random but statistically equivalent microstructures by introducing empirical statistical descriptors into the loss function of deep generative models (e.g., GAN) [52], but then again, it loops back to our original research question: how to select proper descriptors for describing stochastic microstructures without compromising the design freedom.

Design performance: The performances of the optimal designs are influenced by two factors: the accuracy of the microstructure-property surrogate model, and the effectiveness of design exploration/searching in the design spaces generated by each method. Although the curvature functional-based method demonstrates better performances in the presented case study, we should be cautious to make a conclusion. In our previous work [40] and literature [53], it has been demonstrated that training the VAE and the latent variable-property regressor simultaneously can improve the property prediction accuracy. This paper focuses on the capability of learning a unified design space, so the simultaneously training of the latent space and the property repressor is out of scope and not included.

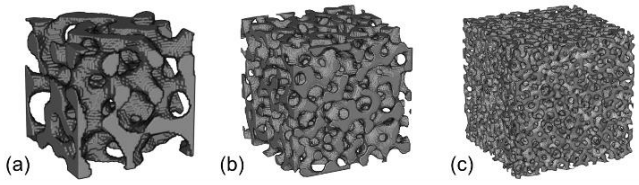

Figure 9: Scalability of the curvature functional-based method: microstructure designs generated from the same design variable vector $\boldsymbol{a}$ = [1, 2.8, 2, -10, -10, 25] and m_0 = -0.25 with sizes of (a) 64^3 (b) 128^3 (c) 256^3 voxels by the curvature functional-based method.

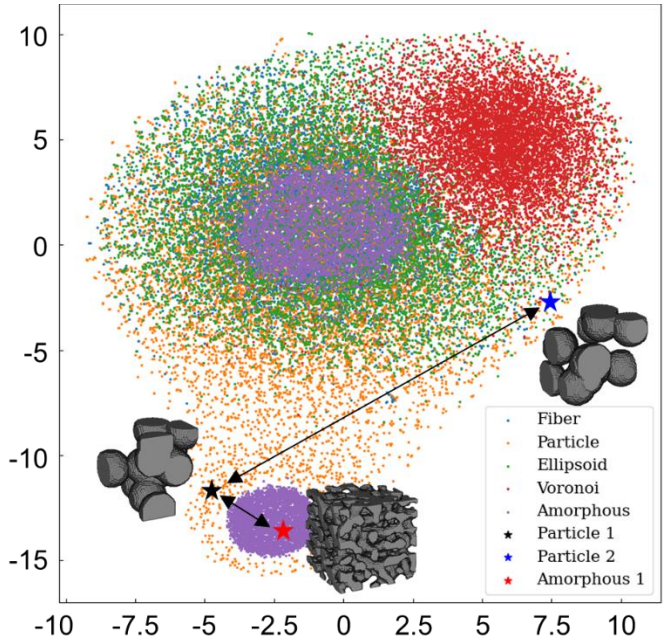

Figure 10: 2D *t*-SNE representations of VAE latent space. It is observed that the distance between two statistically equivalent

random particle microstructures is larger than that between a random particle microstructure and an amorphous microstructure. Therefore, the Euclidean distance in the latent space cannot be used to identify statistically equivalent microstructures.

Table 2: Overview of the comparison between the deep generative model-based and curvature functional-based methods in the design representation. The criterion with * is only valid for the methods and case study presented in this paper and further investigations are needed for other cases. "+" means better, "-" means worse.

Criteria	Deep generative model-based method	Curvature Functional-based method
Computational Cost	−	+
Continuous transition	−	+
Design scalability	−	+
Design diversity	+	−
Dimensionality of the design space	−	+
Interpretability of statistical equivalency	−	+
Design performance*	−	+

6. CONCLUSION AND FUTURE WORK

In this paper, we proposed and compared two methods for generating a unified design space that embodies various categories of stochastic microstructures: the deep generative model-based method and the curvature functional-based method. For the deep generative model-based method, the latent space learned from a highly diversified microstructure database is employed as the microstructure design space. For the curvature functional-based method, the generation parameters in the functionals are used as microstructure design variables. We established surrogate models to predict the relationship between microstructure design variables and the properties of interest, and conducted surrogate model-based optimization to design microstructures for desired properties. Furthermore, we applied the two methods to generate functionally graded structure designs. We present a comprehensive discussion and comparison of each method, outlining their respective advantages and drawbacks. This discussion serves to inform the design process for architecture and composite materials, aiding in the selection of an appropriate method based on the desired outcomes.

In our future work, we plan to test both methods on more engineering case studies to deepen our understanding of the strengths of each method. We are also aiming to extend both methods to the design of 3D mixed-stochasticity microstructural systems that embody both deterministic and stochastic microstructure units.

ACKNOWLEDGEMENT

The authors gratefully acknowledge financial support from the National Science Foundation (CAREER Award CMMI-2142290). L.X. sincerely thanks the insightful discussions with Anna Song at Imperial College London.

REFERENCES

[1] P.P. Meyer, C. Bonatti, T. Tancogne-Dejean, D. Mohr, Graph-based metamaterials: Deep learning of structure-property relations, Materials & Design 223 (2022) 111175.
[2] S. Kumar, S. Tan, L. Zheng, D.M. Kochmann, Inverse-designed spinodoid metamaterials, npj Computational Materials 6(1) (2020) 73.
[3] Z. Wang, W. Xian, M.R. Baccouche, H. Lanzerath, Y. Li, H. Xu, Design of Phononic Bandgap Metamaterials Based on Gaussian Mixture Beta Variational Autoencoder and Iterative Model Updating, Journal of Mechanical Design 144(4) (2022) 041705.
[4] Y. Kim, H.K. Park, J. Jung, P. Asghari-Rad, S. Lee, J.Y. Kim, H.G. Jung, H.S. Kim, Exploration of optimal microstructure and mechanical properties in continuous microstructure space using a variational autoencoder, Materials & Design 202 (2021) 109544.
[5] M. Guo, J. Jiang, Z. Shen, Y. Lin, C.-W. Nan, Y. Shen, High-energy-density ferroelectric polymer nanocomposites for capacitive energy storage: enhanced breakdown strength and improved discharge efficiency, Materials Today 29 (2019) 49-67.
[6] Q. Ye, Y. Liu, H. Lin, M. Li, H. Yang, Multi-band metamaterial absorber made of multi-gap SRRs structure, Applied Physics A 107 (2012) 155-160.
[7] K. Yaji, S. Yamasaki, K. Fujita, Data-driven multifidelity topology design using a deep generative model: Application to forced convection heat transfer problems, Computer Methods in Applied Mechanics and Engineering 388 (2022) 114284.
[8] P. Du, A. Zebrowski, J. Zola, B. Ganapathysubramanian, O. Wodo, Microstructure design using graphs, npj Computational Materials 4(1) (2018) 50.
[9] Y. Li, Z. Chen, L. Su, W. Chen, X. Jin, H. Xu, Stochastic reconstruction and microstructure modeling of SMC chopped fiber composites, Composite Structures 200 (2018) 153-164.
[10] Z. Chen, T. Huang, Y. Shao, Y. Li, H. Xu, K. Avery, D. Zeng, W. Chen, X. Su, Multiscale finite element modeling of sheet molding compound (SMC) composite structure based on stochastic mesostructure reconstruction, Composite Structures 188 (2018) 25-38.
[11] W.M. Tucho, V.H. Lysne, H. Austbø, A. Sjolyst-Kverneland, V. Hansen, Investigation of effects of process parameters on microstructure and hardness of SLM manufactured SS316L, Journal of Alloys and Compounds 740 (2018) 910-925.

[12] S. Wang, J. Ning, L. Zhu, Z. Yang, W. Yan, Y. Dun, P. Xue, P. Xu, S. Bose, A. Bandyopadhyay, Role of porosity defects in metal 3D printing: Formation mechanisms, impacts on properties and mitigation strategies, Materials Today (2022).
[13] T. Tran‐Phu, R. Daiyan, X.M.C. Ta, R. Amal, A. Tricoli, From Stochastic Self‐Assembly of Nanoparticles to Nanostructured (Photo) Electrocatalysts for Renewable Power‐to‐X Applications via Scalable Flame Synthesis, Advanced Functional Materials 32(13) (2022) 2110020.
[14] H. Xu, J. Zhu, D.P. Finegan, H. Zhao, X. Lu, W. Li, N. Hoffman, A. Bertei, P. Shearing, M.Z. Bazant, Guiding the Design of Heterogeneous Electrode Microstructures for Li‐Ion Batteries: Microscopic Imaging, Predictive Modeling, and Machine Learning, Advanced Energy Materials 11(19) (2021) 2003908.
[15] A. Guell Izard, J. Bauer, C. Crook, V. Turlo, L. Valdevit, Ultrahigh energy absorption multifunctional spinodal nanoarchitectures, Small 15(45) (2019) 1903834.
[16] Z. Yang, X. Li, L. Catherine Brinson, A.N. Choudhary, W. Chen, A. Agrawal, Microstructural materials design via deep adversarial learning methodology, Journal of Mechanical Design 140(11) (2018).
[17] C.M. Portela, A. Vidyasagar, S. Krödel, T. Weissenbach, D.W. Yee, J.R. Greer, D.M. Kochmann, Extreme mechanical resilience of self-assembled nanolabyrinthine materials, Proceedings of the National Academy of Sciences 117(11) (2020) 5686-5693.
[18] Y. Li, Z. Chen, H. Xu, J. Dahl, D. Zeng, M. Mirdamadi, X. Su, Modeling and simulation of compression molding process for sheet molding compound (SMC) of chopped carbon fiber composites, SAE International Journal of Materials and Manufacturing 10(2) (2017) 130-137.
[19] Q.T. Do, C.H.P. Nguyen, Y. Choi, Homogenization-based optimum design of additively manufactured Voronoi cellular structures, Additive Manufacturing 45 (2021) 102057.
[20] Y. Jiao, F. Stillinger, S. Torquato, Modeling heterogeneous materials via two-point correlation functions: Basic principles, Physical Review E 76(3) (2007) 031110.
[21] Y. Jiao, F.H. Stillinger, S. Torquato, Modeling heterogeneous materials via two-point correlation functions. II. Algorithmic details and applications, Phys Rev E 77(3) (2008).
[22] S. Torquato, Optimal design of heterogeneous materials, Annu Rev Mater Res 40 (2010) 101-129.
[23] Y. Zhang, M. Yan, Y. Wan, Z. Jiao, Y. Chen, F. Chen, C. Xia, M. Ni, High-throughput 3D reconstruction of stochastic heterogeneous microstructures in energy storage materials, npj Computational Materials 5(1) (2019) 1-8.
[24] S. Yu, C. Wang, Y. Zhang, B. Dong, Z. Jiang, X. Chen, W. Chen, C. Sun, Design of non-deterministic quasi-random nanophotonic structures using Fourier space representations, Scientific reports 7(1) (2017) 1-10.
[25] A. Iyer, R. Dulal, Y. Zhang, U.F. Ghumman, T. Chien, G. Balasubramanian, W. Chen, Designing anisotropic microstructures with spectral density function, Comp Mater Sci 179 (2020) 109559.
[26] M. Grigoriu, Random field models for two-phase microstructures, J Appl Phys 94(6) (2003) 3762-3770.
[27] E. Levina, P.J. Bickel, Texture synthesis and nonparametric resampling of random fields, The Annals of Statistics 34(4) (2006) 1751-1773.
[28] S.G. Advani, C.L. Tucker III, The use of tensors to describe and predict fiber orientation in short fiber composites, Journal of rheology 31(8) (1987) 751-784.
[29] H. Xu, R. Liu, A. Choudhary, W. Chen, A machine learning-based design representation method for designing heterogeneous microstructures, Journal of Mechanical Design 137(5) (2015) 051403.
[30] H. Xu, D.A. Dikin, C. Burkhart, W. Chen, Descriptor-based methodology for statistical characterization and 3D reconstruction of microstructural materials, Comp Mater Sci 85 (2014) 206-216.
[31] Y. Li, H. Xu, W.-J. Lai, Z. Li, X. Su, A Multiscale Material Modeling Approach to Predict the Mechanical Properties of Powder Bed Fusion (PBF) Metal with Consideration of Microstructure Uncertainties, Fourth ASTM Symposium on Structural Integrity of Additive Manufactured Materials & Parts, Oxon Hill, Maryland, USA, 2019.
[32] R.K. Tan, N.L. Zhang, W. Ye, A deep learning–based method for the design of microstructural materials, Structural and Multidisciplinary Optimization 61 (2020) 1417-1438.
[33] R. Bostanabad, Reconstruction of 3d microstructures from 2d images via transfer learning, Computer-Aided Design 128 (2020) 102906.
[34] A. Dahari, S. Kench, I. Squires, S.J. Cooper, Fusion of complementary 2D and 3D mesostructural datasets using generative adversarial networks, Advanced Energy Materials 13(2) (2023) 2202407.
[35] S. Noguchi, J. Inoue, Stochastic characterization and reconstruction of material microstructures for establishment of process-structure-property linkage using the deep generative model, Physical Review E 104(2) (2021) 025302.
[36] S. Kench, S.J. Cooper, Generating three-dimensional structures from a two-dimensional slice with generative adversarial network-based dimensionality expansion, Nature Machine Intelligence 3(4) (2021) 299-305.
[37] R. Cang, Y. Xu, S. Chen, Y. Liu, Y. Jiao, M. Yi Ren, Microstructure representation and reconstruction of heterogeneous materials via deep belief network for computational material design, Journal of Mechanical Design 139(7) (2017).
[38] J. Jung, J.I. Yoon, H.K. Park, H. Jo, H.S. Kim, Microstructure design using machine learning generated low dimensional and continuous design space, Materialia 11 (2020) 100690.
[39] S. Deng, C. Mora, D. Apelian, R. Bostanabad, Data-Driven Calibration of Multifidelity Multiscale Fracture Models Via Latent Map Gaussian Process, Journal of Mechanical Design 145(1) (2023) 011705.
[40] L. Xu, N. Hoffman, Z. Wang, H. Xu, Harnessing structural stochasticity in the computational discovery and design of microstructures, Materials & Design 223 (2022) 111223.

[41] Y. Li, W. Chen, H. Xu, X. Jin, 3D representative volume element reconstruction of fiber composites via orientation tensor and substructure features, 31st Annual Technical Conference of the American Society for Composites, American Society for Composites, 2016.
[42] N. Hoffman, J. Lee, W. Li, J. Zhu, H. Xu, A Stochastic Microstructure Reconstruction-Based Mechanical and Transport Modeling Approachfor Learning the Microstructure-Property Relationship of Li-Ion Battery Graphite Anodes, 239th ECS meeting, Digital Meeting, 2021.
[43] R. Cang, H. Li, H. Yao, Y. Jiao, Y. Ren, Improving direct physical properties prediction of heterogeneous materials from imaging data via convolutional neural network and a morphology-aware generative model, Comp Mater Sci 150 (2018) 212-221.
[44] N. Dilokthanakul, P.A. Mediano, M. Garnelo, M.C. Lee, H. Salimbeni, K. Arulkumaran, M. Shanahan, Deep unsupervised clustering with gaussian mixture variational autoencoders, arXiv preprint arXiv:1611.02648 (2016).
[45] K. Deb, A. Pratap, S. Agarwal, T. Meyarivan, A fast and elitist multiobjective genetic algorithm: NSGA-II, IEEE transactions on evolutionary computation 6(2) (2002) 182-197.
[46] K. Shoemake, Animating rotation with quaternion curves, Proceedings of the 12th annual conference on Computer graphics and interactive techniques, 1985, pp. 245-254.
[47] A. Song, Generation of tubular and membranous shape textures with curvature functionals, Journal of Mathematical Imaging and Vision 64(1) (2022) 17-40.
[48] P.-A. Geslin, I. McCue, B. Gaskey, J. Erlebacher, A. Karma, Topology-generating interfacial pattern formation during liquid metal dealloying, Nature communications 6(1) (2015) 8887.
[49] D. Montes de Oca Zapiain, J.A. Stewart, R. Dingreville, Accelerating phase-field-based microstructure evolution predictions via surrogate models trained by machine learning methods, npj Computational Materials 7(1) (2021) 3.
[50] F.V. Senhora, E.D. Sanders, G.H. Paulino, Optimally‐Tailored Spinodal Architected Materials for Multiscale Design and Manufacturing, Advanced Materials 34(26) (2022) 2109304.
[51] A. Gayon-Lombardo, L. Mosser, N.P. Brandon, S.J. Cooper, Pores for thought: generative adversarial networks for stochastic reconstruction of 3D multi-phase electrode microstructures with periodic boundaries, npj Computational Materials 6(1) (2020) 1-11.
[52] F. Zhang, Q. Teng, H. Chen, X. He, X. Dong, Slice-to-voxel stochastic reconstructions on porous media with hybrid deep generative model, Comp Mater Sci 186 (2021) 110018.
[53] L. Wang, Y.-C. Chan, F. Ahmed, Z. Liu, P. Zhu, W. Chen, Deep generative modeling for mechanistic-based learning and design of metamaterial systems, Comput Method Appl M 372 (2020) 113377.